

A novel design of a low-voltage low-loss T-match RF-MEMS capacitive switch

Li-Ya Ma¹ · Anis Nurashikin Nordin² · Norhayati Soin¹

Received: 31 August 2016 / Accepted: 6 October 2017 / Published online: 10 November 2017
© Springer-Verlag GmbH Germany 2017

Abstract This paper presents a novel design, optimization and analysis of capacitive radio frequency (RF) micro-electromechanical system (MEMS) switch. The design incorporates a novel membrane and beams' structure with two short high-impedance transmission-line (T-line) sections added on either side of the switch (namely T-match switch) to improve its RF performance, while maintaining low-actuation voltage. The short high-impedance T-line section has narrower width and higher impedance than the coplanar waveguide (CPW)'s signal line, behaves as series inductor to compensate the switch's up-state capacitance and provides excellent matching at the design frequency. This high-impedance T-line section was designed, simulated and optimized using finite-element-modelling (FEM) tool of electromagnetic (EM) simulator of AWR Design EnvironmentTM. The optimized T-line section's width and length is 10 μm and 70 μm , respectively. The RF-MEMS switch is actuated by electrostatic force with low-actuation voltage of 2.9 V, has maximum von Mises stress of 13.208 MPa which is less than aluminium's yield stress and can be operated in robust conditions. Compared to the normal capacitive RF-MEMS switch, this T-match capacitive RF-MEMS switch with two sections of optimized high-impedance T line has improved the performance of return loss and insertion loss, at switch-on state, by 45.83% and 55.35%, respectively; while at the switch-off state, the isolation is increased by 24.05%; only the switch-off return loss is degraded by 11.7% but the value (-0.5519 dB) is still located in the range of design specifications. The RF-MEMS

switch's actuation time was simulated to be ~ 27 μs with amplitude of 5 V up-step voltage.

1 Introduction

Low-cost radio frequency (RF) micro-electro-mechanical system (MEMS) switches are prime candidates to replace the conventional GaAs FET and p-i-n diode switches in microwave and millimetre-wave communication systems, mainly due to their low insertion loss, good isolation, linear characteristic and small power consumption (Balaraman et al. 2002; Fouladi and Mansour 2010). These MEMS devices can be designed and fabricated by techniques similar to those of very large scale integrated (VLSI) circuits using surface or bulk micromachining that can be manufactured by traditional batch-processing method. Previous researchers have proposed diverse designs of RF-MEMS switch in the past few decades using different structures or actuation mechanisms (Fouladi and Mansour 2010; Badia et al. 2012; Kim 2012; Mahameed and Rebeiz 2011). The RF-MEMS switches can be implemented into a number of RF applications, systems or subsystems, such as MEMS phase shifters, voltage controlled oscillators, filters, power amplifiers, matching networks, very high or ultra-high frequency switchable radio front-end circuits, digitized capacitor banks and reconfigurable antennas (Rebeiz 2003).

RF-MEMS switches are devices that are mechanically opening or shorting the transmission line (T line) using an actuation mechanism. Electrostatic force is the most prevalent technique in use today due to its simple structure, compatibility with the integrated circuits fabrication process, and virtually zero power consumption compared to other available actuation mechanisms (Persano et al. 2015;

✉ Li-Ya Ma
maliya8445@gmail.com

¹ University of Malaya, Kuala Lumpur, Malaysia

² International Islamic University Malaysia, Kuala Lumpur, Malaysia

Reddy and Shanmuganatham 2014). In 2010, a capacitive RF-MEMS switch with two metal-dielectric warped membranes was presented and fabricated in standard 0.35 μm complementary metal–oxide–semiconductor (CMOS) process, where insertion loss of -0.98 dB and return loss of -13 dB at 20 GHz was achieved with actuation voltage of 68 V (Fouladi and Mansour 2010). Another electrostatically driven RF-MEMS switch using robust single-crystal silicon was designed by Kim et al. (2010), where pull-in voltage of 10 V, insertion loss of -0.2 dB, and isolation of -23.57 dB at 15 GHz was achieved. In Mahameed and Rebeiz's paper (2011), a metal-based shunt capacitive RF-MEMS switch was developed; and it has an insertion loss of -0.11 dB, return loss of -26.27 dB at 25 GHz with pull-in voltage of 12.75 V. High actuation voltages is one of the biggest drawbacks for electrostatically actuated RF-MEMS switches that prevents them from being directly integrated in standard CMOS chip systems which usually have operating voltage of 3.3 V (Ma et al. 2016a).

Pull-in voltage (V_p) for a capacitive RF-MEMS switch can be calculated using Eq. (1) as follows:

$$V_p = \sqrt{\frac{8kg_0^3}{27\epsilon_0 A}} \quad (1)$$

where k is the spring constant of the moving part; g_0 is the initial gap between the two electrodes; ϵ_0 is the permittivity of air, 8.854×10^{-12} F/m; and A is the actuation area.

Based on (1) (Ya et al. 2014), there are several methods which can be used to reduce the value of V_p ; (1) reducing the spring constant of the moving-electrode part (e.g. beam or membrane) (Peroulis et al. 2003; Guo et al. 2003; Dai and Chen 2006; Afrang and Abbaspour-Sani 2006), (2) increasing the switch's actuation area (Kim et al. 2010; Peroulis et al. 2003), (3) using very high dielectric constant materials for the dielectric layer (Badia et al. 2012), and (4) reducing the air gap between two electrodes (Guo et al. 2003; Afrang and Abbaspour-Sani 2006). For most standard CMOS process or CMOS-compatible processes, silicon dioxide (SiO_2) or silicon nitride (Si_3N_4) are the only choices for the dielectric layer material (Guo et al. 2003; Dai and Chen 2006); therefore it is not possible to employ the very high dielectric constant materials in the switch design. The low-spring-constant structure can achieve low V_p ; however the penalty paid is very long switching time and high stress distribution on the suspended parts (Peroulis et al. 2003). Having large actuation areas and small air gap can also reduce V_p ; however, it will increase the up-state capacitance and further to degrade the up-state return loss. Thus, there are design trade-offs between having low spring constants, short switching time, small moving part

stress distribution, and large actuation area to achieve a robust low-voltage RF-MEMS switch (Ma et al. 2016a).

The capacitive RF-MEMS switch's down-state capacitance over up-state capacitance is the capacitance ratio of the switch which can be calculated by (2). Capacitance ratio is an important design parameter for the capacitive switch, since the higher capacitance ratio can promise a better RF performance, vice versa.

$$C_{ratio} = \frac{C_d}{C_u} \approx \frac{g_0\epsilon_r + t_d}{(1+x)t_d} \quad (2)$$

where, ϵ_r and t_d is the permittivity and thickness of dielectric layer, respectively; C_d and C_u is down-state and up-state capacitance, respectively; and x is a coefficient of fringing field capacitance ($= 0.3-0.4$).

A problem of (Ma et al. 2016a) and other CMOS-compatible low-voltage capacitive switch designs (Kim et al. 2010; Dai and Chen 2006; Afrang and Abbaspour-Sani 2006) is that a large capacitance ratio (e.g. ≥ 100), which can be obtained by (2) (Rebeiz 2003), cannot be achieved due to the low dielectric constant and a common low-voltage design range of the air gap (1.5–3 μm). This results in a high up-state capacitance and therefore high return losses (Rebeiz 2003). T-match circuits provide an excellent solution to reduce up-state return loss by compensate the high up-state capacitance with two short high-impedance sections of T line (Rebeiz 2003). Usage of the T-match technique to improve the performance of RF-MEMS switch is relatively novel and not much research has been dedicated to it so far.

In this paper, a RF-MEMS capacitive switch with low actuation-voltage of 2.9 V is proposed while the structure can be operated in its elastic range. In order to improve the RF-MEMS switch's RF performance, specifically the return loss of switch-on state, two short high-impedance T-line sections are added before and after the RF-MEMS switch. The rest of the paper is divided into the following sections: Sect. 2 presents the design of low-voltage low-loss T-match RF-MEMS switch where the design specifications, working principle, details of the structures for low-actuation voltage, optimization of the high-impedance T-line sections for low loss, and electrical modelling are illustrated. Section 3 shows the finite element modelling (FEM) simulations and discussion, where the electro-mechanical properties and RF performance of the normal RF-MEMS switch and T-match RF-MEMS switch are displayed. The conclusion provides a comparison of state-of-the-art designs of the electrostatic-actuated capacitive RF-MEMS switches with our work.

2 Design of low-voltage low-loss T-match RF-MEMS switch

In this section, a novel structure for low-voltage and low-loss T-match RF-MEMS switch is proposed, as shown in Fig. 1. Two short high-impedance T-line sections have been optimized and added to the low-voltage RF-MEMS switch as shown in Fig. 1b, where W_{hi} and L_{hi} is the width and length of the high-impedance T-line section, respectively. The electrical modelling circuit of the T-match RF-MEMS switch is explained. Figure 2 shows the low-voltage low-loss T-match RF-MEMS switch’s design methodology.

2.1 Design specifications and working principle

The design specifications for the capacitive shunt RF-MEMS switch is listed in Table 1, where the V_p of less than 3.3 V is aimed for directly implementation with the most CMOS integrated circuit (IC) designs; an up-state return loss (S_{11up}) of less than -10 dB can guarantee a good match of the input with the switch (Rebeiz 2003);

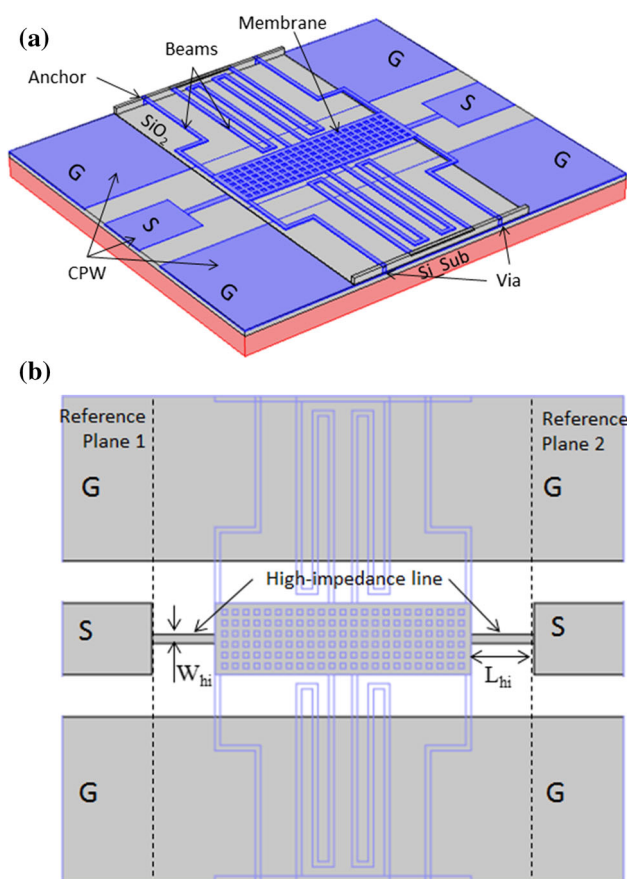


Fig. 1 T-match capacitive RF-MEMS switch. **a** Overall view of the switch design, **b** top view of RF-MEMS switch with two high-impedance T-line sections

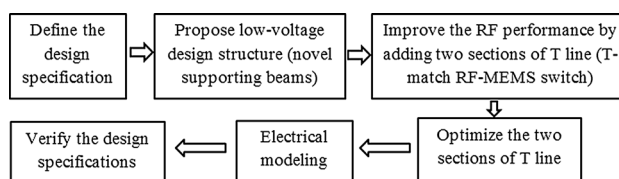


Fig. 2 Design methodology

large capacitance ratio (> 40) can produce good RF performance.

A RF-MEMS capacitive shunt switch basically contains three parts, namely coplanar waveguide (CPW), a thin dielectric layer and a top electrode which can be membrane, cantilever or fixed beam. There is a DC bias voltage supplied to the capacitor’s two electrodes to actuate or release the top movable electrode and further to turn on or turn off the switch. When the bias voltage is increased to a certain value which can pull the top electrode down to the CPW line, it is called the switch’s pull-in voltage (V_p); and the switch is turned off. Once the bias voltage is reduced to almost zero volt, the top electrode will be rebounded back to the original position and the switch is turned on.

2.2 Low-voltage RF-MEMS switch

Figure 3 shows the design of the low-voltage RF-MEMS capacitive switch. There are four folded beams to support a big membrane which are also connected to the ground planes by via. Another two spring beams located at each side of the signal line are used to support the middle part of the membrane and also supply the DC bias voltage to the membrane. The signal line is kept at DC ground potential. In order to reduce the substrate loss, a high resistivity (> 10 k Ω -cm) silicon substrate with thickness of 500 μ m is chosen.

The switch’s dimensions are summarized in Table 2, where t_m , t_d , t_{CPW} is the thickness of membrane, thin dielectric layer and CPW line, respectively; and g_0 is the initial gap between two electrodes. The CPW’s $G/W/G$ (G is the gap between the signal line and ground plane and W is the width of the signal line) set to be 47 μ m/80 μ m/47 μ m is in order to obtain a 50- Ω T line. These dimensions have been optimized in previous work as shown in Ma et al. (2016a). The folded beams and spring beams are used to largely reduce the total spring constant of the membrane structure which is simulated around 0.22 N/m and further to get a low actuation voltage. The electro-mechanical properties of the structure are displayed in Sect. 3.1.

Table 1 Design specifications

Parameter	Value (or type)	Parameter	Value (or type)
V_P	≤ 3.3 V (Reddy and Shanmuganatham 2014)	Actuation mechanism	Electrostatic
Insertion loss ($S_{21_{up}}$) and down-state return loss ($S_{11_{down}}$)	> -1 dB (Fouladi and Mansour 2010; Kim et al. 2010; Ma et al. 2016a; Ya et al. 2014)	Circuit configuration	Shunt connection
Isolation ($S_{21_{down}}$)	< -15 dB (Fouladi and Mansour 2010; Kim et al. 2010; Ma et al. 2016a)	Contact type	Capacitive
Up-state return loss ($S_{11_{up}}$)	< -10 dB (Rebeiz 2003)	Frequency	K band
Capacitance ratio (C_{Ratio})	> 40 (Rebeiz 2003)	Up-state capacitance (C_u)	0.05–0.2 pF (Rebeiz 2003)

Fig. 3 **a** Overall view of RF-MEMS capacitive switch design, **b** cross-section view of the switch (A–A')

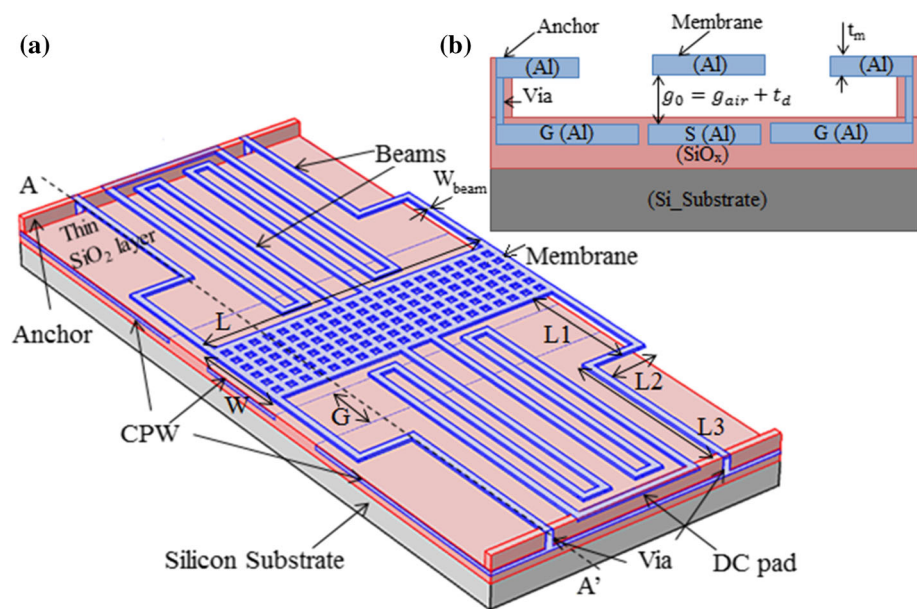


Table 2 RF-MEMS switch's physical dimensions

Parameter	Metal thickness and air gap				Membrane and CPW			Beams			
	t_m	t_d	t_{CPW}	g_0	W	L	G	L_1	L_2	L_3	W_{beam}
Values (μm)	1	0.15	1	3	80	280	47	80	50	150	6

2.3 T-match RF-MEMS switch

The large membrane used in the RF-MEMS switch produces 50 to 100 fF up-state capacitance. When compared with the design of small membrane and up-state capacitance of less than 10 fF ($C_u < 10$ fF), the RF-MEMS switch's insertion loss is degraded about 0.5–1 dB. And then the switch-on-state return loss is less than 10 dB for K-band RF-MEMS switch. All these characteristics do not comply with the design specifications of Table 1. In this work, to meet the required design specifications, we propose the addition of two high-impedance T-line sections

before and after the switch, as shown in Fig. 1b. The T-line sections behave as series inductors to provide an excellent match at the design frequency which is called a T-match circuit (Wang et al. 2010).

As displayed in Fig. 1b, the high-impedance T-line section's length and width are labelled as L_{hi} and W_{hi} , respectively. To determine the values of L_{hi} and W_{hi} , an optimization method based on the switch's RF performance simulations has been done by EM simulator of AWR Design Environment™. Table 3 shows the S parameters' simulation of the RF-MEMS switch with two high-impedance T-line sections, where W_{hi} was varied

Table 3 S parameters of RF-MEMS switch with different dimensions of high-impedance T-line sections (W_{hi} = 10–40 μm ; L_{hi} = 20–150 μm)

W_{hi} (μm)	S parameters and resonant frequency	L_{hi} (μm)			
		20	50	100	150
	f_r	21 GHz	20 GHz	20 GHz	19 GHz
10	$S11_{up}$ (dB)	- 9.534	- 11.09	- 11.26	- 11.1
	$S21_{up}$ (dB)	- 0.4225	- 0.2586	- 0.2891	- 0.6494
	$S11_{down}$ (dB)	- 0.7538	- 0.5614	- 0.5431	- 0.6494
	$S21_{down}$ (dB)	- 24.08	- 25.94	- 27.86	- 29.1
20	$S11_{up}$ (dB)	- 9.273	- 10.51	- 10.26	- 10
	$S21_{up}$ (dB)	- 0.4379	- 0.2807	- 0.3308	- 0.7026
	$S11_{down}$ (dB)	- 0.7248	- 0.5215	- 0.4853	- 0.6082
	$S21_{down}$ (dB)	- 24.02	- 25.92	- 27.34	- 28.3
30	$S11_{up}$ (dB)	- 9.117	- 10.14	- 9.758	- 9.286
	$S21_{up}$ (dB)	- 0.4526	- 0.3016	- 0.4013	- 0.7696
	$S11_{down}$ (dB)	- 0.7124	- 0.4959	- 0.5007	- 0.5874
	$S21_{down}$ (dB)	- 23.96	- 26.04	- 25.97	- 27.07
40	$S11_{up}$ (dB)	- 8.981	- 9.886	- 9.268	- 8.776
	$S21_{up}$ (dB)	- 0.464	- 0.322	- 0.4543	- 0.8348
	$S11_{down}$ (dB)	- 0.7061	- 0.4859	- 0.4901	- 0.5808
	$S21_{down}$ (dB)	- 23.98	- 25.96	- 25.73	- 26.91

f_r is the LC resonant frequency resulted by switch’s LCR model, where the best isolation can be found
 Bold italic values indicate better results than other conditions

from 10 to 40 μm and L_{hi} was varied from 20 to 150 μm . The investigated S parameters were between reference plane 1 and 2, as shown in Fig. 1b.

The range of L_{hi} is from 20 to 150 μm which is basically determined by the up-state return loss’s simulation results; the maximum up-state return loss is appeared in this range. And the range of W_{hi} (10–40 μm) is determined by fabrication limitations (minimum fabrication mask design is 10 μm), the requirement of the T line’s high impedance (> 50 Ω) and design specification of $S11_{up} < - 10$ dB. Figure 4 illustrates the simulation of CPW’s impedance under different T line’s widths using TXLINE 2003[®]. From this plot, it can be seen that, the narrower T line, the higher impedance is produced.

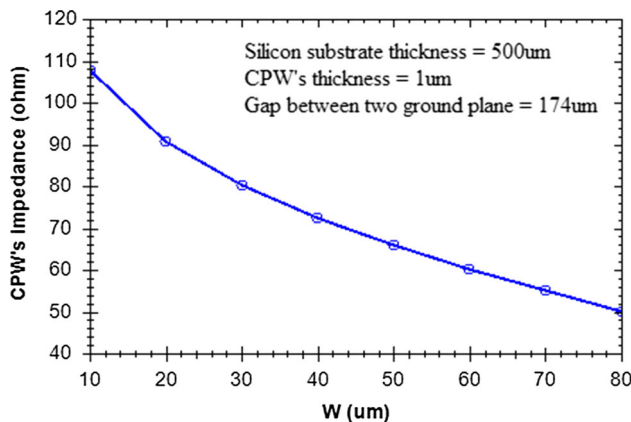


Fig. 4 Relationship of CPW’s impedance and its T line’s width

All the simulated S parameters within the setting of L_{hi} and W_{hi} has been summarized in Table 3; it can be seen that: (1) the length of the high-impedance T-line section can control the LC resonant frequency (f_r) of the switch; with longer T-line section, the smaller f_r is obtained; (2) with narrower T line, the better S parameters can be obtained; however, the minimum of W_{hi} is limited with fabrication process’ resolution; (3) the best RF performance is located between 50 and 100 μm of L_{hi} while W_{hi} equals to 10 μm .

Therefore, a finer simulation for L_{hi} from 50 to 100 μm was done further, as shown in Table 4; it can be seen that: (1) when L_{hi} is ranging from 70 to 80 μm , the value of $S11_{up}$ is the lowest ($S11_{up} = - 11.35$ dB < - 10 dB); (2) the highest $S21_{up}$ ($S21_{up} = - 0.2527$ dB) is appeared at L_{hi} equals to 70 μm . Since the high-impedance T-line sections are used to compensate the up-state capacitance; L_{hi} of 70 μm is chosen. Moreover when W_{hi} equals to 10 μm and L_{hi} is 70 μm , the values of $S11_{down}$ and $S21_{down}$ are fulfilled the requirements of the design specifications.

2.4 Electrical modelling

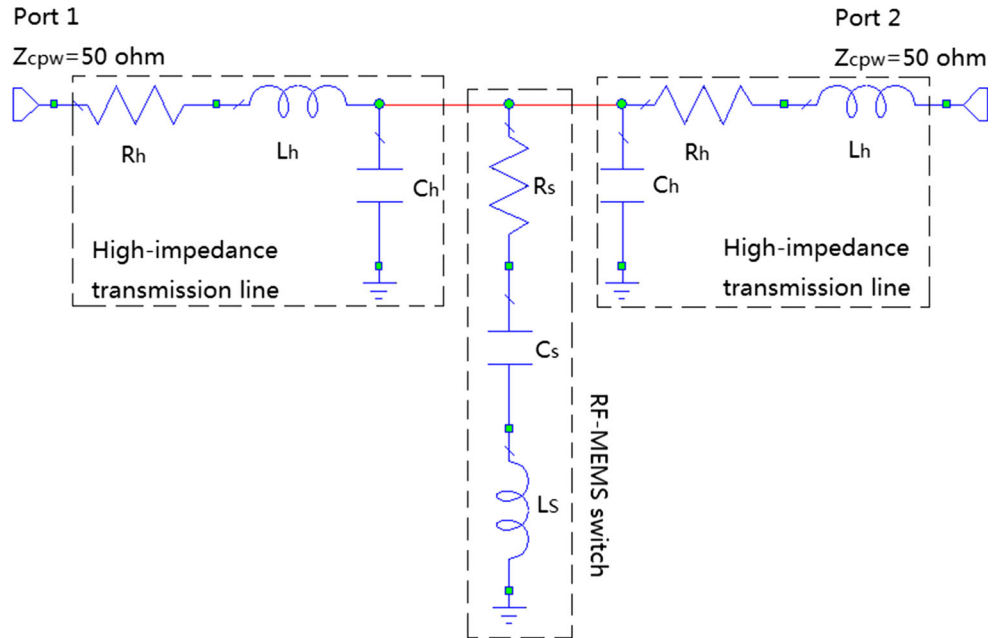
The RCL equivalent circuit of the T-match capacitive RF-MEMS switch is displayed in Fig. 5. The series resistance (R_h), inductance (L_h), and shunt capacitance (C_h) is the equivalent lumped elements of the high-impedance T-line section, respectively; C_s , L_s , and R_s are the RF-MEMS switch’s equivalent lumped elements, where C_s can be

Table 4 S parameters of RF-MEMS switch with different dimensions of high-impedance T-line sections ($W_{hi} = 10 \mu\text{m}$; $L_{hi} = 50\text{--}100 \mu\text{m}$)

S parameters @ $f_r = 20 \text{ GHz}$	$L_{hi} (\mu\text{m})$					
	50	60	70	80	90	100
$S11_{up}$ (dB)	- 11.09	- 11.22	- 11.35	- 11.35	- 11.32	- 11.26
$S21_{up}$ (dB)	- 0.2586	- 0.2581	- 0.2527	- 0.2681	- 0.2752	- 0.2891
$S11_{down}$ (dB)	- 0.5614	- 0.5575	- 0.5519	- 0.554	- 0.5506	- 0.5431
$S21_{down}$ (dB)	- 25.94	- 26.7	- 27.44	- 27.84	- 27.95	- 27.86

f_r is the LC resonant frequency resulted by switch’s LCR model, where the best isolation can be found
 Bold italic values indicate better results than other conditions

Fig. 5 Equivalent circuit of the T-match capacitive RF-MEMS switch



equalled to C_d or C_u according to the switch’s operating state.

The values of all the lumped elements were derived and obtained basically from the FEM simulation results. The impedance of the capacitive RF-MEMS switch (Z_S) (without two high-impedance T-line sections) can be approximated by (3) (Rebeiz 2003).

$$Z_S = R_S + j\omega L_S + \frac{1}{j\omega C_S} = \begin{cases} \frac{1}{j\omega C_S} & \leftarrow f \ll f_r \\ R_S & \leftarrow f = f_r \\ j\omega L_S & \leftarrow f \gg f_r \end{cases} \quad (3)$$

$$f_r = \frac{1}{2\pi \sqrt{L_S C_d}} \quad (4)$$

$$C_d = \frac{\epsilon_0 \epsilon_r A}{t_d} \quad (5)$$

where, the LC series resonant frequency (f_r) and down-state capacitance (C_d) can be calculated by (4) and (5) (Rebeiz 2003); f is the switch’s operating frequency.

The values of L_h , R_h , and C_h can be extracted by simulating the T-match RF-MEMS switch’s S parameters or characteristic impedance in EM simulator, as shown the final equivalent lumped parameter’s values of the T-match RF-MEMS capacitive switch in Table 5. By another way, if the high-impedance T-line sections are considered as an ideal inductor, its inductance and the impedance of the added T line can be estimated using (6) and (7) (Ma et al. 2016b). For the condition of $C_u = 89 \text{ fF}$, $Z_0 = 50 \Omega$ at frequency of 20 GHz, the calculated inductance of high-impedance T-line section is 122 pH and its length is 223 μm with fixed impedance of 65 Ω . The reasons for the difference existing between the calculated and simulated lumped elements’ values can be summarized into following several points: (1) the calculation model for (6) is ideal and did not consider the shunt capacitance and series resistance of the high-impedance T-line section; (2) in (Rebeiz 2003), it was mentioned that even though (6) can be used to estimate the value of the high-impedance T line’s inductance, the solution will not be a perfect match; (3) in (7),

Table 5 Equivalent lumped parameters' value of the T-match RF-MEMS switch

Parameter	L_h (pH)	R_h (Ω)	C_h (fF)	L_s (pH)	R_s (Ω)	C_s (pF)
Value	225	0.5	57.5	11.69	1.958	$C_u = 0.089, C_d = 5.16$

the impedance's calculation of the high-impedance T-line section only considers the length of the T line, however, its width also has a large effect on its impedance which can be seen from Fig. 4. Therefore, comparing with the simulation model which considers the width and length's effect of the high-impedance T-line sections simultaneously and simulation results, the modelling equations of (6) and (7) can only give a very rough estimation for the lumped elements' values. The equivalent lumped-element values extracted from simulation model matches well with the corresponding 3D structure; this can be seen from Fig. 6, where the characteristic impedance of both the equivalent circuit and 3D structure were presented.

$$L_h = \frac{1 \pm \sqrt{1 - (\omega C_u Z_0)^2}}{\omega^2 C_u} \tag{6}$$

$$Z_h = \frac{L_h c}{L_{hi} \sqrt{\epsilon_{eff}}} \tag{7}$$

$$C_u = \frac{\epsilon_0 A}{g_0 + \frac{L_u}{\epsilon_r}} \tag{8}$$

where Z_0 is RF transmission line's standard impedance (50 Ω); C_u is the up-state capacitance and can be calculated

by (8); Z_h and L_{hi} is the impedance and length of the added T-line sections; ϵ_{eff} is the relative effective dielectric constant of the T line which is about 6.3 for silicon substrate; g_0 is the gap between two electrodes; and c is the speed of the light in free space (3×10^8 m/s).

3 FEM simulations and discussion

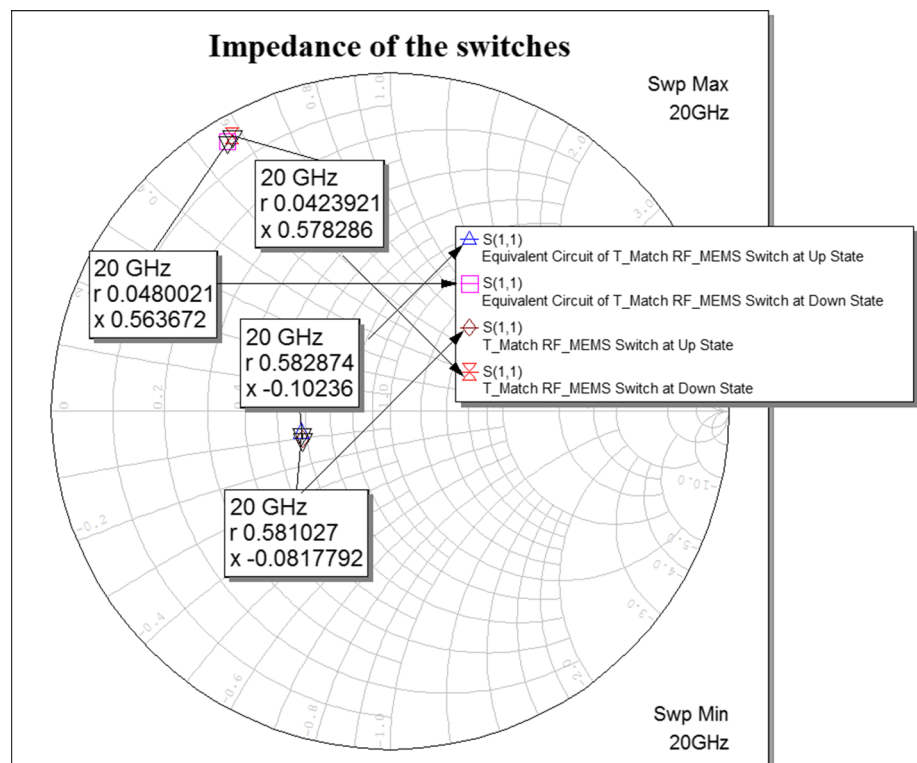
The developed RF-MEMS switch's electro-mechanical properties, RF performance, as well as the improved low-loss design have been verified in this section by using FEM simulations in each different field.

3.1 Electro-mechanical properties of the RF-MEMS switch

The simulation model is established in accordance with the dimensions in Table 2 and estimated by Comsol Multiphysics® simulations in each different field.

Figure 7 shows the simulated total spring constant of the RF-MEMS switch is 0.22 N/m, which is reciprocal of the vertical displacement's slope. It also can be seen that, when the membrane is pulled down to the maximum air gap of

Fig. 6 Impedance comparison of the T-match RF-MEMS switch's equivalent circuit and 3D structure



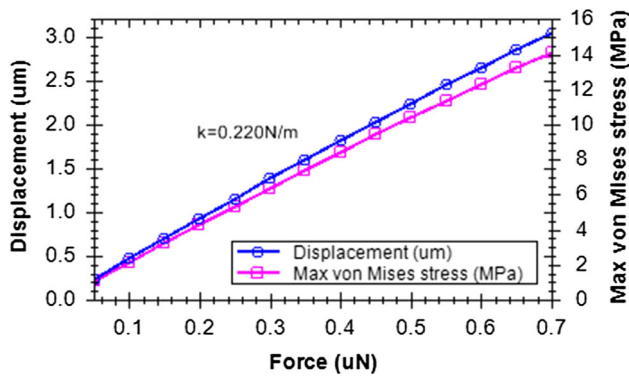


Fig. 7 RF-MEMS switch's spring constant and maximum von Mises stress

$2.85 \mu\text{m}$, the maximum von Mises stress is much less than the aluminium's yield stress of 124 MPa (Dai and Chen 2007); therefore the motion of the membrane and beams can be operated in its elastic range; the structure is stable and robust. The 3D view of the membrane's displacement and von Mises stress distribution at the actuated state is displayed in Fig. 8.

The simulated 1st resonant frequency or eigen frequency of the membrane and beams' structure is 6.984 kHz . By using Eq. (9) (Rebeiz 2003), the calculated 1st resonant frequency is 7.8 kHz which almost agrees with the simulation result.

$$\omega_0 = \sqrt{k/m} = 2\pi f_{r1} \quad (9)$$

where, k is the total spring constant (0.22 N/m); m is the mass of the membrane and beams (namely, $9.139\text{E}-11 \text{ kg}$); and ω_0 (or f_{r1}) is the 1st resonant frequency of the membrane and beams' structure.

The quality factor of the RF-MEMS switch can be estimated by using (10) (Rebeiz 2003) which is a first-order approximation for the quality factor of a fixed–fixed beam. The calculated quality factor for the designed RF-MEMS switch is 0.158 . This value is less than 0.5 which results in a slow switching time (Rebeiz 2003), as shown in Fig. 9b, which is around $27 \mu\text{s}$. If the membrane's thickness is increased to $1.4 \mu\text{m}$ and air gap is increased to $3.5 \mu\text{m}$, a quality factor of 0.574 will be obtained which is an advantageous condition in practice, as mentioned in Rebeiz (2003); however, it will increase the actuation voltage around 2.2 times.

$$Q = \frac{\sqrt{E\rho}t^2}{\mu\left(\frac{WL}{2}\right)^2} g_0^3 \quad (10)$$

where, $E = 70 \text{ GPa}$ and $\rho = 2700 \text{ kg/m}^3$ is the Young's modulus and density of the aluminum, respectively; $t_m = 1 \mu\text{m}$, $W = 80 \mu\text{m}$ and $L = 280 \mu\text{m}$ is the thickness, width and length of the membrane, respectively; $g_0 = 2.85 \mu\text{m}$ is the air gap of the two electrodes; and $\mu = 0.87 \times 1.845 \times 10^{-5} \text{ Pa s}$ is the effective viscosity of air (Rebeiz 2003).

In dynamic domain, the RF-MEMS switch's actuation voltage and switching time has been simulated and verified by Comsol's electromechanics model, as displayed in Fig. 9. The simulated pull-in voltage of 2.2 V , comparing with the calculated value of 2.9 V , is a bit smaller which is because of the finite mesh element size used in the simulation. A time dependent simulation was conducted to estimate the actuation time. With a step-up voltage load, amplitude of 5 V and rising time of $1 \mu\text{s}$, the actuation time of $27 \mu\text{s}$ is obtained as shown in Fig. 9b. This actuation time depends strongly on the applied voltage since the

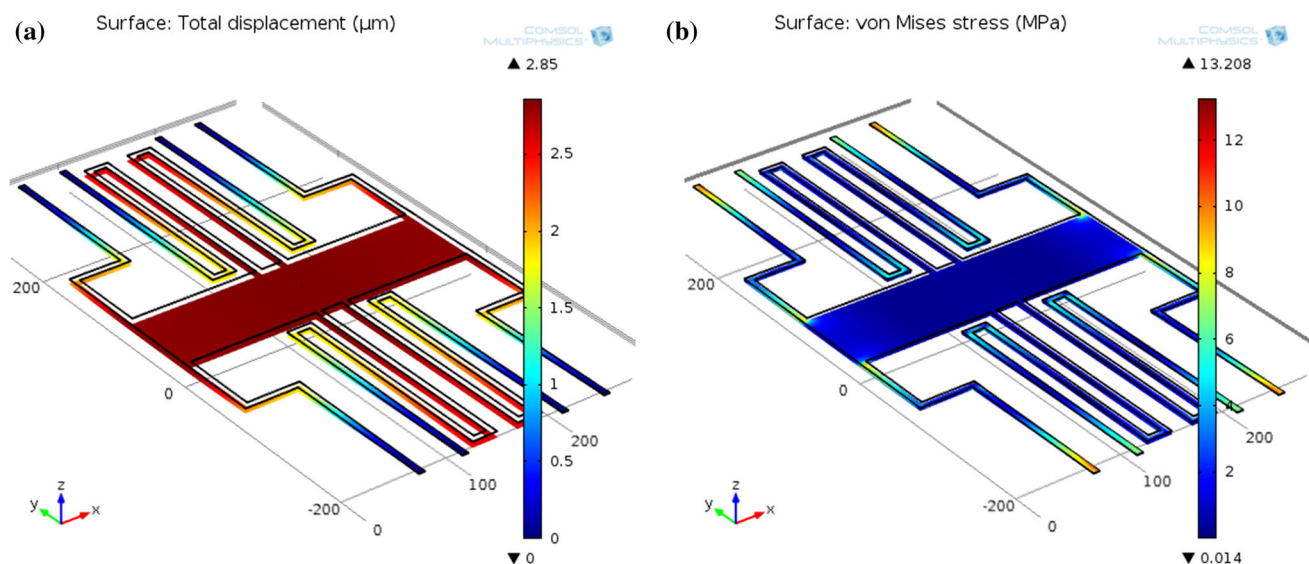
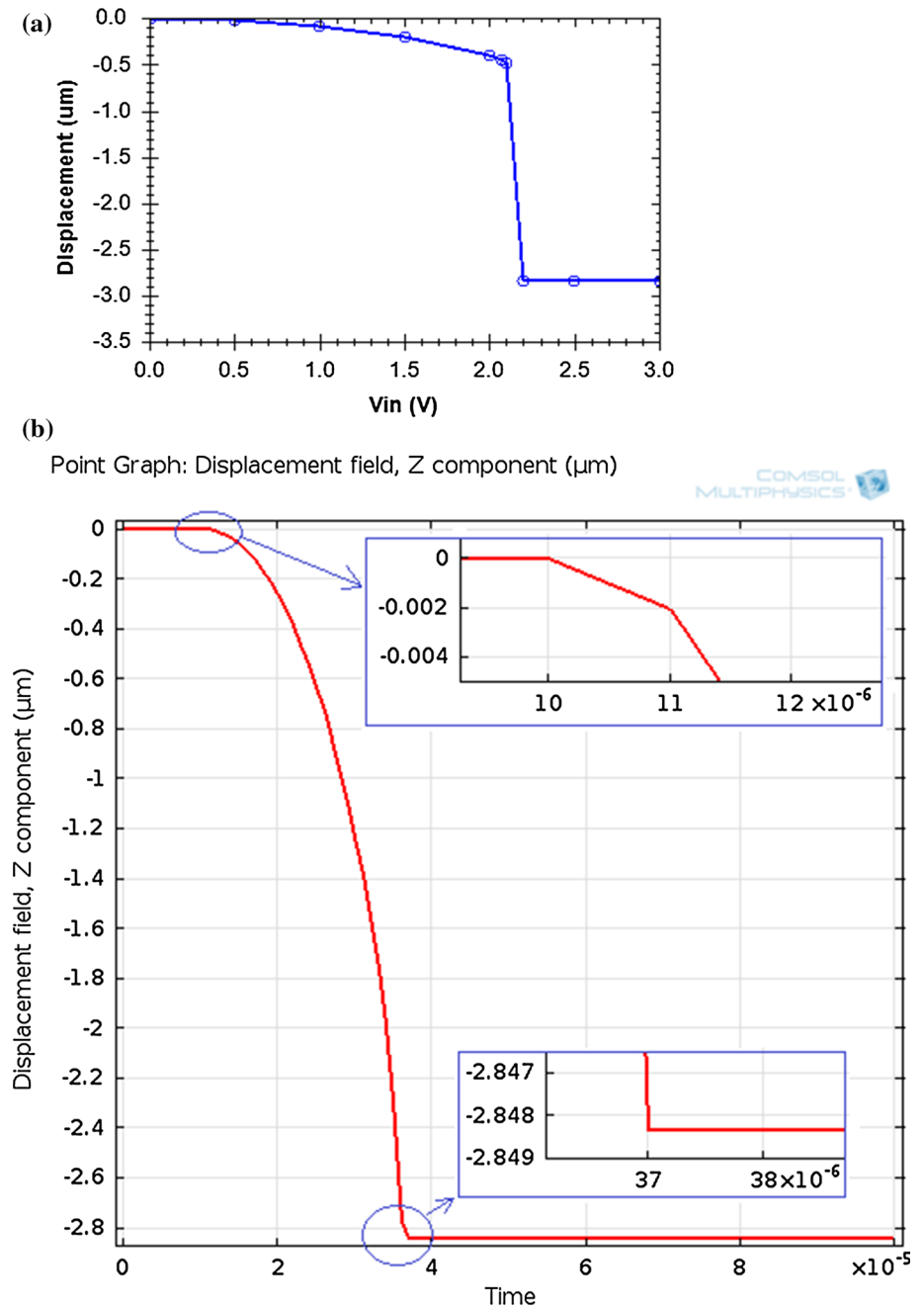


Fig. 8 3D view of the RF-MEMS switch's actuated state, **a** membrane's displacement; **b** Von Mises stress distribution

Fig. 9 RF-MEMS switch's dynamic simulations, **a** pull-in voltage; **b** actuation time



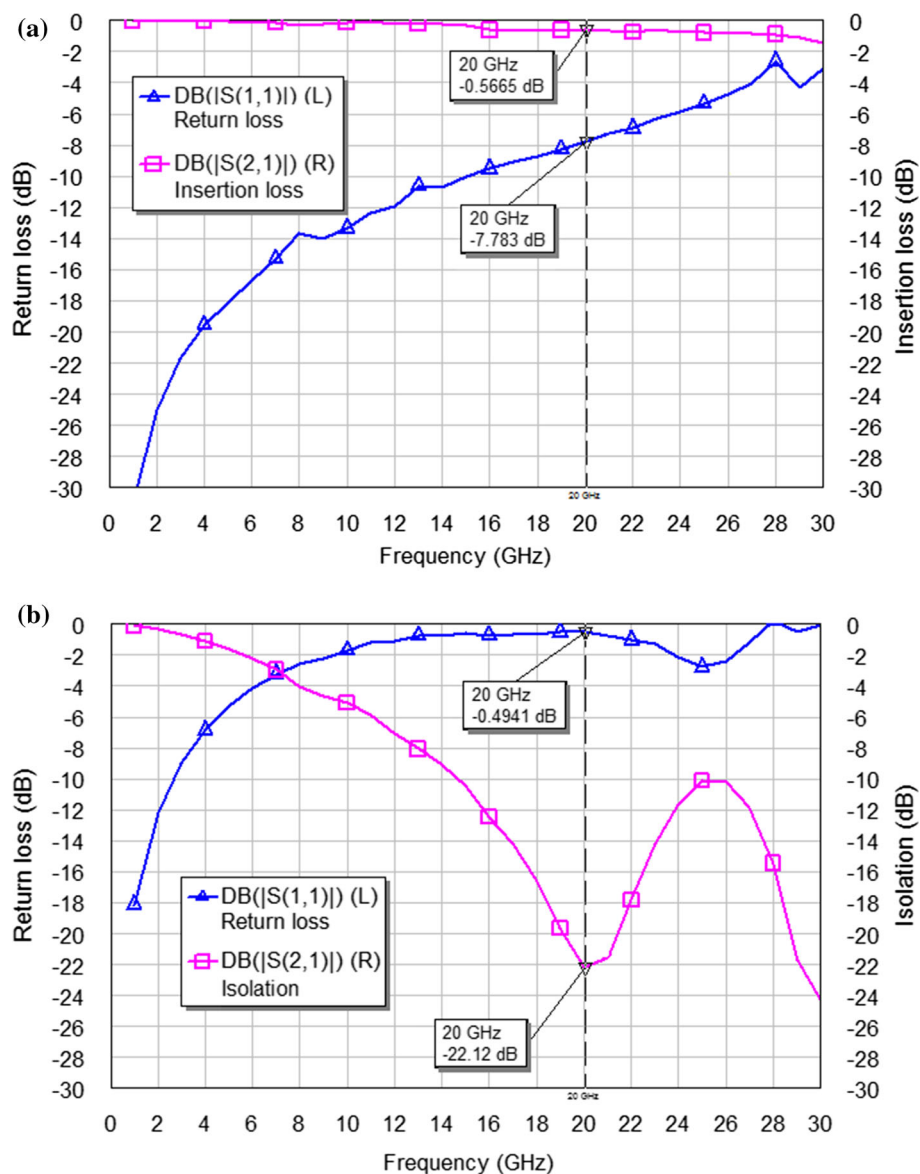
larger the voltage, the stronger the electrostatic force (Rebeiz 2003). Here the ratio of applied voltage over actuation voltage is around 1.7.

3.2 RF performance of the RF-MEMS switch without high-impedance T line

Electromagnetic (EM) simulator from AWR[®] software has been used to compute the RF performance (S

parameters) of the RF-MEMS switch. For EM evaluations, the switch is considered from a digital point of view; only the membrane's initial and final positions are studied without dynamical considerations (such as actuation speed and gas damping contributions) since the switch-on and switch-off states are the only data necessary for evaluating the overall device RF performances (Bartolucci et al. 2012). The simulated S parameters are presented in Fig. 10, where the LC resonant frequency

Fig. 10 Simulated S parameters of the RF-MEMS switch, **a** switch-on state; **b** switch-off state



(f_r) of the RF-MEMS switch is located at 20 GHz. When the switch is turned on, the return loss ($S_{11_{up}}$) and insertion loss ($S_{21_{up}}$) is -7.783 dB and -0.566 dB, respectively, at the frequency of 20 GHz; when the switch is turned off, return loss ($S_{11_{down}}$) and isolation ($S_{21_{down}}$) is -0.4941 dB and -22.12 dB, respectively, at 20 GHz. The switch-on (or up-state) return loss is higher than -10 dB which is not satisfied with the design specification (< -10 dB); however it can be improved by the additional high-impedance T-line sections, as shown the simulation results in the next section.

3.3 Improved RF performance with two high-impedance T lines

The improved RF-MEMS switch model with two sections of high-impedance T line has been simulated using EM simulator. As specified in Sect. 2.3, a range of high-impedance T-line section with W_{hi} of $10\text{--}40$ μm and L_{hi} of $20\text{--}150$ μm has been investigated. The relationships of the simulated S parameters with W_{hi} and L_{hi} are displayed in Fig. 11. Figure 11a describes the simulation results of up-state return loss ($S_{11_{up}}$); when W_{hi} is reduced, the $S_{11_{up}}$ is

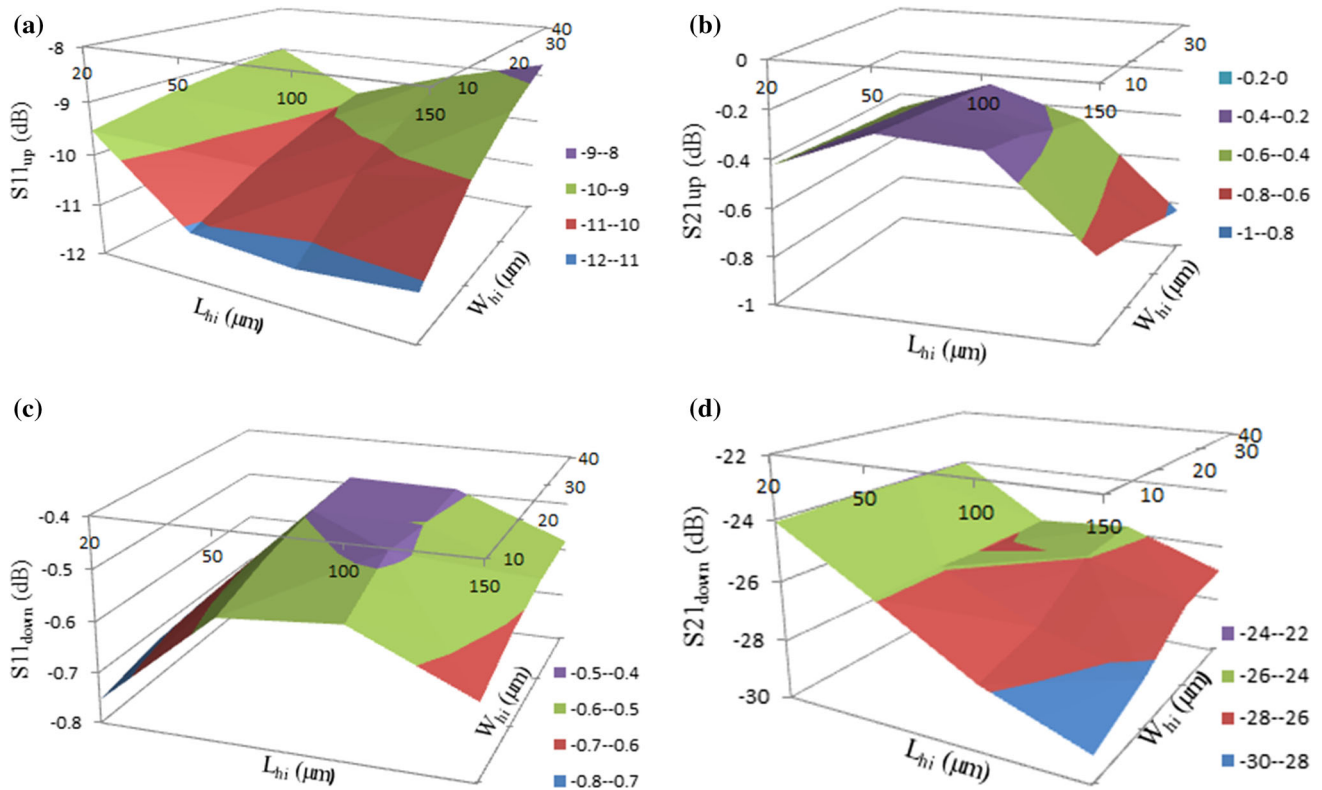


Fig. 11 Simulated S parameters of the T-match RF-MEMS switch with $W_{hi} = 10\text{--}40\ \mu\text{m}$ and $L_{hi} = 20\text{--}150\ \mu\text{m}$

decreased; and optimum values (namely $S11_{up} < -10\ \text{dB}$) located at W_{hi} is $10\ \mu\text{m}$ and L_{hi} is from 50 to $100\ \mu\text{m}$. Figure 11b–d shows that all the simulated values have met the design specifications, namely, the insertion loss ($S21_{up}$) and switch-off (or down-state) return loss ($S11_{down}$) is higher than $-1\ \text{dB}$; and isolation ($S21_{down}$) is less than $-15\ \text{dB}$.

Figure 12 shows the relationship of S parameters and L_{hi} with the fixed W_{hi} . In Fig. 12a, it shows that, high-impedance T-line sections can increase the up-state return loss ($S11_{up}$) a lot. Comparing with the original low-voltage RF-MEMS switch, the T-match RF-MEMS switch with T-line sections of $W_{hi} = 10\ \mu\text{m}$ and $L_{hi} = 70\ \mu\text{m}$ can increase the up-state return loss 45.83% to $-11.35\ \text{dB}$ which fulfils the design specification. With the same T-line sections, meantime, insertion loss and isolation can be improved by 55.35% and 24.05%, respectively. Except for the return loss at switch-off state, it degrades about 11.7%. But all the S parameters are located within the design requirements of $S11_{up} < -10\ \text{dB}$, $S21_{up}$ and $S11_{down} > -1\ \text{dB}$, and $S21_{down} < -15\ \text{dB}$. The impedance of the high-impedance T-line section, RF-MEMS switch, as well as the

T-match RF-MEMS switch has been simulated also and presented in Fig. 13. Figure 13a shows the impedance of the T-line section ($W_{hi} = 10\ \mu\text{m}$ and $L_{hi} = 70\ \mu\text{m}$) is about $61\ \Omega$ (point B). Figure 13b shows the high-impedance T-line section as series inductor can compensate capacitance a lot at both switch-on and switch-off state.

4 Conclusion

In this paper, a shunt capacitive RF-MEMS switch with novel structure is designed and simulated. The RF-MEMS switch has a very low actuation voltage of $2.9\ \text{V}$ which is compatible with most standard CMOS and integrated circuits. In order to improve the RF-MEMS switch’s RF performance to meet the design specifications, a T-match circuit with two high-impedance T-line sections added before and after the switch is proposed. By FEM simulations and optimization with a series of T-line dimensions, two width of $10\ \mu\text{m}$ and length of $70\ \mu\text{m}$ T-line sections with the impedance of $61\ \Omega$ can promote a relative good RF response. Comparing with the original RF performance

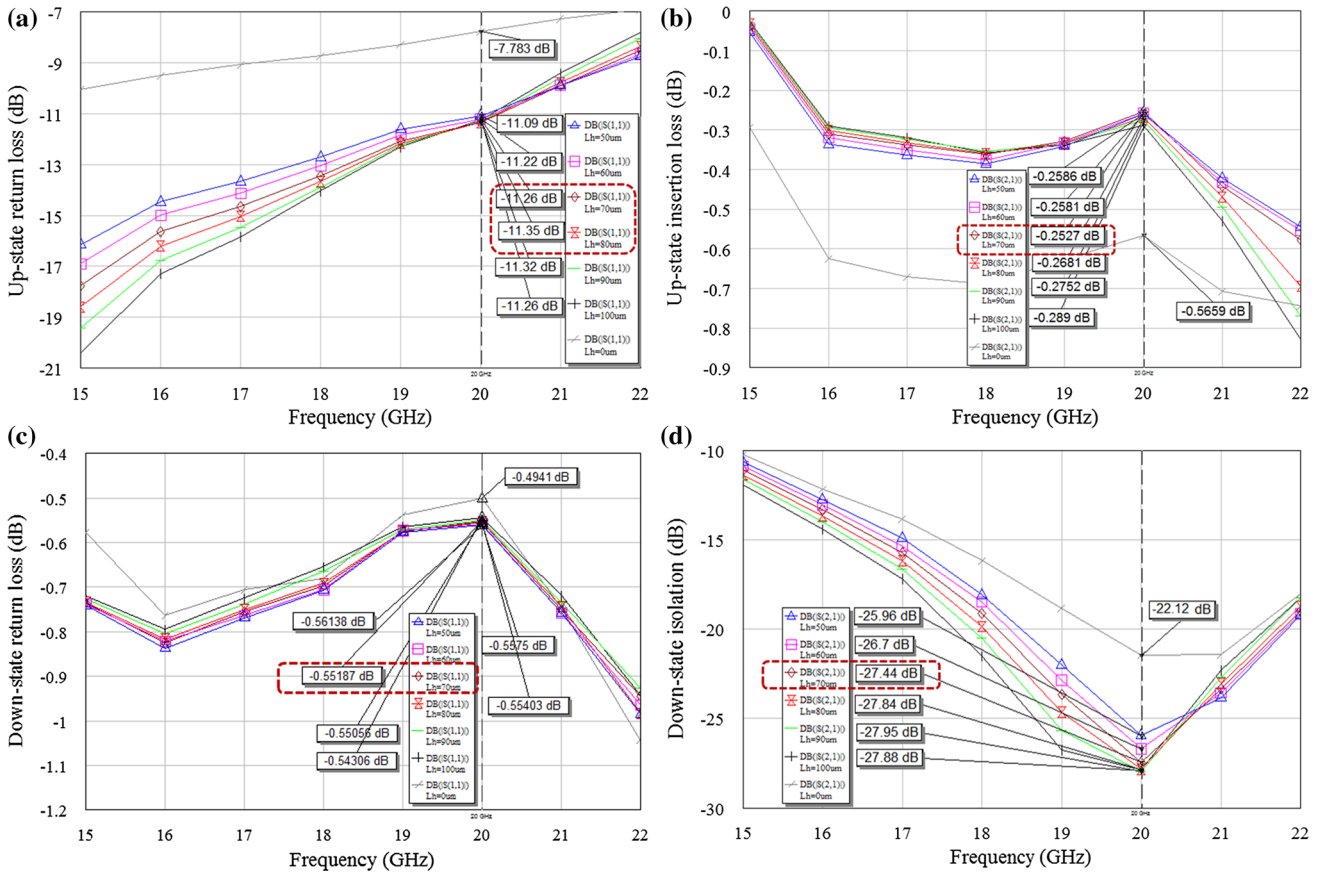


Fig. 12 RF performance of the T-match RF-MEMS switch with $W_{hi} = 10 \mu\text{m}$

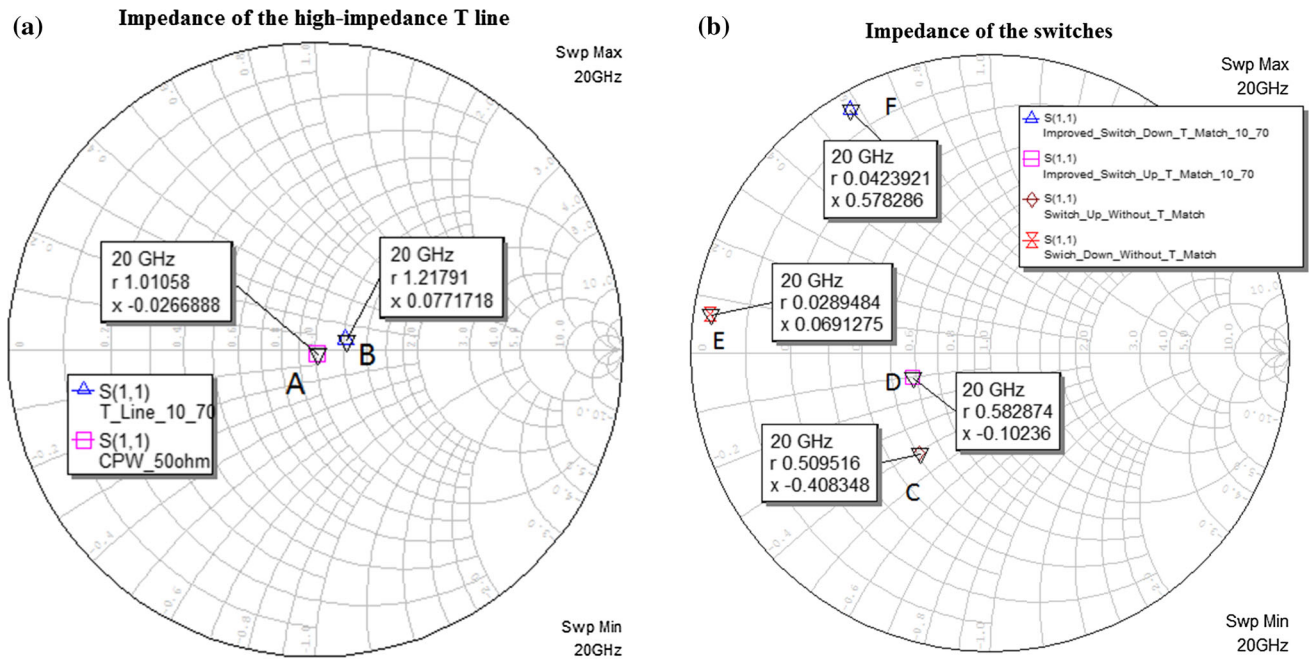
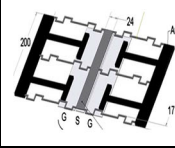
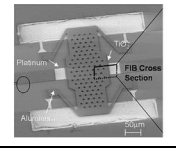
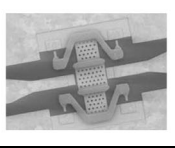
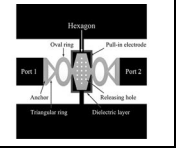
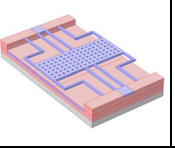
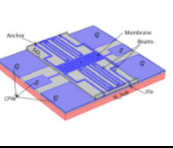


Fig. 13 Impedance in Smith chart, a impedance of the T-line section; b impedance of the switches

Table 6 Comparison of state-of-the-art RF-MEMS capacitive switches

Electrostatic switch	Dai et al., 2006, [14]	Ferna et al., 2008, [20]	Badia et al., 2012, [3]	Deng et al., 2015, [21]	Li-Ya Ma et al., 2015, [10]	This work
Structure						
V_p	7V	8V	21.8V	16V	3.04V	2.2V(simulate) 2.9V(calculate)
S_{11up}	-10dB @40GHz	---	-9.23dB @40GHz	---	-5.65dB @40GHz	-11.35dB @20GHz
S_{21up}	-3.1dB @40GHz	>-0.5dB @20GHz	-0.68dB @40GHz	-3dB @50GHz	-1.51dB @40GHz	-0.2527dB @20GHz
S_{11down}	---	---	---	---	-0.6dB @40GHz	-0.5519dB @20GHz
S_{21down}	-15dB @40GHz	<-20dB @20GHz	-35.8dB @40GHz	-19dB @50GHz	-24.38dB @40GHz	-27.44dB @20GHz
$C_{Ratio} (C_d/C_u) (F)$	13.4 (0.15p/11.2f)	196 (10p/60f)	9.87 (1.27p/0.128f)	6.8 (0.34p/55f)	52 (7.31p/0.14p)	60 (5.16p/85f)
Actuation Time	8.2μs	---	---	---	13.5μs	27μs
Remarks	TSMC0.35μm CMOS + Maskless post-process	Six-mask process	The design uses seven-mask process and has relative high actuation voltage	MEMS surface micromaching process	The design has poor RF performance at switch-on state since the low-resistivity silicon substrate used	The design has very low actuation voltage and good RF responses

of the low-voltage RF-MEMS switch; the developed T-match RF-MEMS switch can improve the up-state return loss, insertion loss and isolation by 45.83%, 55.35%, and 24.05%, respectively. A comparison of the proposed T-match RF-MEMS switch with other state-of-the-art designs which use electrostatic actuation mechanism and implement by capacitive contact with CPW line is presented in the end of the paper (in Table 6).

Acknowledgements The research is collaborative effort between University of Malaya and International Islamic University Malaysia. All authors would like to thank the financial support by the RACE fund (RACE12-006-0006), UM CR 004-2013, and University Malaya High Impact Research Grant (UM.C/HIR/MOHE/ENG/19).

References

Afrang S, Abbaspour-Sani E (2006) A low voltage MEMS structure for RF capacitive switches. *Prog Electromagn Res* 65:157–167. doi:10.2528/PIER06093001

Badia MFB, Buitrago E, Ionescu AM (2012) RF MEMS shunt capacitive switches using AlN compared to dielectric.

J Microelectromech Syst 21(5):1229–1240. doi:10.1109/JMEMS.2012.2203101

Balaraman D, Bhattacharya SK, Ayazi F, Papapolymerou J (2002) Low-cost low actuation voltage copper RF MEMS switches. In: 2002 IEEE MTT-S international microwave symposium digest, vol 2, pp 1225–1228. doi:10.1109/MWSYM.2002.1011879

Bartolucci G, Angelis GD, Lucibello A, Marcelli R, Proietti E (2012) Analytic modelling of RF MEMS shunt connected capacitive switches. *J Electromagn Waves Appl* 26(8–9):1168–1179. doi:10.1080/09205071.2012.710564

Dai CL, Chen JH (2006) Low voltage actuated RF micromechanical switches fabricated using CMOS-MEMS technique. *Microsyst Technol* 12(12):1143–1151. doi:10.1007/s00542-006-0243-7

Dai CL, Chen YL (2007) Modelling and manufacturing of micromechanical RF switch with inductors. *Sensors* 7(11):2660–2670. doi:10.3390/s7112670

Deng Z, Wei H, Fan S, Gan J (2016) Design and analysis a novel RF MEMS switched capacitor for low pull-in voltage application. *Microsyst Technol* 22(8):2141–2149. doi:10.1007/s00542-015-2604-6

Fernández-Bolaños M, Perruisseau-Carrier J, Dainesi P, Ionescu AM (2008) RF MEMS capacitive switch on semi-suspended CPW using low-loss high-resistivity silicon substrate. *Microelectron Eng* 85(5):1039–1042. doi:10.1016/j.mee.2008.01.093

Fouladi S, Mansour RR (2010) Capacitive RF MEMS switches fabricated in standard 0.35-CMOS technology. *IEEE Trans*

- Microw Theory Tech 58(2):478–486. doi:[10.1109/TMTT.2009.2038446](https://doi.org/10.1109/TMTT.2009.2038446)
- Guo FM, Zhu ZQ, Long YF, Wang WM, Zhu SZ, Lai ZS, Lu W (2003) Study on low voltage actuated MEMS rf capacitive switches. *Sens Actuators A* 108(1):128–133. doi:[10.1016/S0924-4247\(03\)00372-8](https://doi.org/10.1016/S0924-4247(03)00372-8)
- Kim CH (2012) Mechanically coupled low-voltage electrostatic resistive RF multithrow switch. *IEEE Trans Industr Electron* 59(2):1114–1122. doi:[10.1109/TIE.2011.2159694](https://doi.org/10.1109/TIE.2011.2159694)
- Kim JM, Lee S, Park JH, Baek CW, Kwon Y, Kim YK (2010) Electrostatically driven low-voltage micromechanical RF switches using robust single-crystal silicon actuators. *J Micromech Microeng* 20(9):095007. doi:[10.1088/0960-1317/20/9/095007](https://doi.org/10.1088/0960-1317/20/9/095007)
- Ma LY, Nordin AN, Soin N (2016a) Design, optimization and simulation of a low-voltage shunt capacitive RF-MEMS switch. *Microsyst Technol* 22(3):537–549. doi:[10.1007/s00542-015-2585-5](https://doi.org/10.1007/s00542-015-2585-5)
- Ma LY, Soin N, Nordin AN (2016) A novel design of low-voltage low-loss K-band RF-MEMS capacitive switch. In: 2016 IEEE symposium on design, test, integration and packaging of MEMS/MOEMS (DTIP), pp 1–5. doi:[10.1109/DTIP.2016.7514827](https://doi.org/10.1109/DTIP.2016.7514827)
- Mahameed R, Rebeiz GM (2011) RF MEMS capacitive switches for wide temperature range applications using a standard thin-film process. *IEEE Trans Microw Theory Tech* 59(7):1746–1752. doi:[10.1109/TMTT.2011.2135376](https://doi.org/10.1109/TMTT.2011.2135376)
- Peroulis D, Pacheco SP, Sarabandi K, Katehi LP (2003) Electromechanical considerations in developing low-voltage RF MEMS switches. *IEEE Trans Microw Theory Tech* 51(1):259–270. doi:[10.1109/TMTT.2002.806514](https://doi.org/10.1109/TMTT.2002.806514)
- Persano A, Quaranta F, Martucci MC, Siciliano P, Cola A (2015) On the electrostatic actuation of capacitive RF MEMS switches on GaAs substrate. *Sens Actuators A* 232:202–207. doi:[10.1016/j.sna.2015.05.008](https://doi.org/10.1016/j.sna.2015.05.008)
- Rebeiz GM (2003) RF MEMS. Theory, design, and technology. Wiley, Hoboken, p 6 (pp. **92**, **228**, **66**)
- Reddy BL, Shanmuganatham T (2014) Design of novel capacitive RF MEMS shunt switch with aluminum nitride (AlN) dielectric. *Proc Mater Sci* 6:692–700. doi:[10.1016/j.mspro.2014.07.085](https://doi.org/10.1016/j.mspro.2014.07.085)
- Wang Z, Liu Z, Li X (2010) A Ka-band 3-bit RF MEMS switched line phase shifter implemented in coplanar waveguide. In: 2010 10th IEEE international conference on solid-state and integrated circuit technology (ICSICT), pp 1450–1452. doi:[10.1109/ICSICT.2010.5667567](https://doi.org/10.1109/ICSICT.2010.5667567)
- Ya ML, Soin N, Nordin AN (2014) Novel low-voltage RF-MEMS switch: design and simulation. In: 2014 IEEE international conference on semiconductor electronics (ICSE), pp 142–145. doi:[10.1109/SMELEC.2014.6920816](https://doi.org/10.1109/SMELEC.2014.6920816)